$$\cdot \left\{ \frac{mA_3}{\left(\frac{m\pi}{2}\right)^2 - u^2} - \frac{nA_4}{\left(\frac{n\pi}{2}\right)^2 - u^2} \right\} e^{-j(kR-u)}, \quad (67)$$

and in the E plane ($\phi = \pi/2$)

$$E_\theta = \frac{-j^m \sin\left(\frac{m\pi}{2}\right) ab}{\lambda\pi R} \left\{ \frac{A_5}{m} - \frac{A_6}{n} \right\} \frac{\sin u'}{u'} e^{-j(kR-u')} \quad (68)$$

$$E_\phi = \frac{-j^m \sin\left(\frac{m\pi}{2}\right) ab}{\lambda\pi R} \left\{ \frac{A_7}{m} - \frac{A_8}{n} \right\} \frac{\sin u'}{u'} e^{-j(kR-u')} \quad (69)$$

where

$$A_1 = j \frac{Ca}{m\pi} (\beta + \omega\epsilon\eta \cos\theta) \quad (70)$$

$$A_2 = j \frac{Ca}{n\pi} (\beta + \omega\epsilon\eta \cos\theta) \quad (71)$$

$$A_3 = \frac{Ca}{m\pi\kappa} \left\{ \frac{\eta}{\omega} \left[\left(\frac{m\pi}{2}\right)^2 - N \right] + \frac{\mu \cos\theta}{\beta} \left[\left(\frac{m\pi}{a}\right)^2 - M \right] \right\} \quad (72)$$

$$A_4 = \frac{Ca}{n\pi\kappa} \left\{ \frac{\eta}{\omega} \left[\left(\frac{n\pi}{a}\right)^2 - N \right] + \frac{\mu \cos\theta}{\beta} \left[\left(\frac{n\pi}{a}\right)^2 - M \right] \right\} \quad (73)$$

$$A_5 = \frac{Ca}{m\pi\kappa} \left\{ \frac{\mu}{\beta} \left[\left(\frac{m\pi}{a}\right)^2 - M \right] + \frac{\eta \cos\theta}{\omega} \left[\left(\frac{m\pi}{a}\right)^2 - N \right] \right\} \quad (74)$$

$$A_6 = \frac{Ca}{m\pi\kappa} \left\{ \frac{\mu}{\beta} \left[\left(\frac{n\pi}{a}\right)^2 - M \right] + \frac{\eta \cos\theta}{\omega} \left[\left(\frac{n\pi}{a}\right)^2 - N \right] \right\} \quad (75)$$

$$A_7 = \frac{jCa}{m\pi} (\beta \cos\theta + \eta\omega\epsilon) \quad (76)$$

$$A_8 = \frac{jCa}{n\pi} (\beta \cos\theta + \eta\omega\epsilon). \quad (77)$$

Acknowledgment

Grateful acknowledgment is made to the Boeing Airplane Company for the permission to use the digital computer facilities for most of the computations involved in the text. Thanks are also extended to Carl G. Lindell for computer programming and to K. W. Osborne for lettering and inking the drawings.

Launching Efficiency of Wires and Slots for a Dielectric Rod Waveguide*

R. H. DuHAMEL† AND J. W. DUNCAN‡

Summary—This paper describes an experimental investigation of surface wave launching efficiency. Wires, rings, and slots are considered as exciters of the HE_{11} mode on a dielectric rod image line. A formula is derived which relates the efficiency of a launcher to its impedance as a scatterer on the surface waveguide. Efficiency is obtained by using this formula and also by applying Deschamps' method for determining the scattering matrix coefficients of a two-port junction. Graphs are presented which illustrate the variation of efficiency with the dimensions of the launchers and with the parameter λ_g/λ, the ratio of the guide wavelength to the free space wavelength.

* Manuscript received by the PGMTT, August 1, 1957; revised manuscript received January 28, 1958. The work described in this paper was supported by Wright Air Dev. Ctr. under Contract No. AF 33(616)-3220, and is an abstract of Antenna Lab. Tech. Rep. No. 24, Electrical Engineering Research Lab., Engineering Experiment Station, University of Illinois, Urbana, Ill. The paper was presented at the IRE WESCON, Los Angeles, Calif., August 23, 1956.

† Collins Radio Co., Cedar Rapids, Iowa.
‡ Dept. of Elec. Eng., University of Illinois, Urbana, Ill.

Introduction

THE THEORY of wave propagation on dielectric rods has been treated extensively by a number of investigators [1]–[3]. In recent years the dielectric rod waveguide has been employed with considerable success as a dielectric antenna [4], [5]. The mode which is most often used for dielectric rod antennas is the HE_{11} (or dipole) mode. It is the lowest order mode which can propagate on a dielectric rod and has no

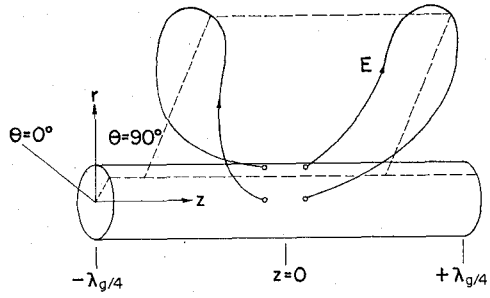

Fig. 1—Typical electric field line of dipole mode on a dielectric rod.

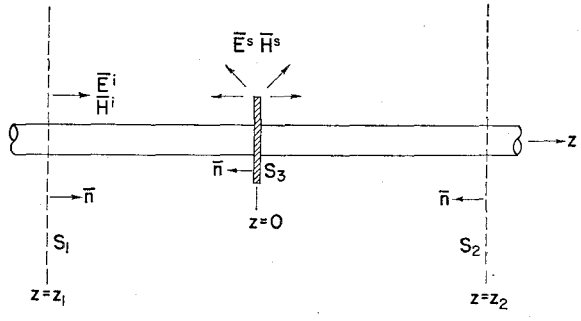

Fig. 2—Surface waveguide and scatterer.

cutoff frequency. Very little information appears in the literature on methods of launching the dipole mode on a rod. The dielectric rod antenna is usually excited from closed metal waveguide or a horn. It appears that the first experimental study of dipole mode launching efficiency was conducted by Margerum at Northwestern University [6]. He measured the launching efficiency of circular metal waveguide which was excited in the TE_{11} mode. Recently, King and Schlesinger measured the radiation loss from a circular aperture in a thin metal sheet placed on a dielectric image line [7]. The purpose of this work was twofold. First, a new method of measuring launching efficiency was investigated and compared with a conventional method. The new method requires a measurement of the impedance that the launcher presents to a surface waveguide when used as a scatterer. The efficiency is simply related to this impedance. With this technique, it is relatively easy to study the variation of launching efficiency with the dimensions of the launcher and the parameter λ_g/λ. Although this method was used only with the dielectric image line, it may be applied to other types of surface waveguides. The second purpose of this work was to investigate various types of simple wire and slot launchers. Curves showing the variation of launching efficiency with launcher dimensions and the parameter λ_g/λ are presented.

The Dielectric Image Line

The characteristics of dielectric rod propagation and the dipole mode will be briefly reviewed. The HE_{11} mode is an asymmetric, hybrid mode which has components of both the electric and magnetic field in the direction of propagation. A typical electric field line outside the rod is shown in Fig. 1 [8]. The cutoff wavelength of a mode is a function of the rod radius b, and free space wavelength λ [3]. For a polystyrene rod with dielectric constant $\epsilon = 2.5$, higher order modes can propagate only when the rod diameter exceeds 0.626λ. The ratio λ_g/λ is a function of the parameter b/λ [3], [5]. As b/λ approaches zero, λ_g/λ approaches unity and most of the power is propagated in the space surrounding the rod. The transverse field distribution of the dipole mode is such that a metal sheet may be passed through the axis of the rod without disturbing the field. A half-round rod mounted on a metal ground plane is the dielectric image line first proposed by King [9], who has developed various circuit components for the dielectric image line and describes a conical horn and parabolic reflector as transitions from image line to closed waveguide [10]. It is possible to measure standing waves along the image line by means of a slotted section in the ground plane [10]; thus, the impedance of a scatterer may be readily determined.[1] In this paper an expression is derived which relates the efficiency of a launcher to its impedance as a scatterer on the surface waveguide.

Launching Efficiency from the Scatterer Impedance

Referring to Fig. 2, consider a cylindrical surface waveguide of arbitrary cross section. The guide is assumed lossless with a surface wave $\bar{E}^i$, $\bar{H}^i$ incident from the left and a perfectly conducting scatterer, denoted as surface S_3, located at $z=0$. The surfaces S_1 and S_2 are infinite transverse planes normal to the z axis located at $z=z_1$ and $z=z_2$, respectively.

The incident surface wave will induce a current on the scatterer which will produce a scattered field that consists of guided waves to the left and right plus a radiation field. An expression for the reflection coefficient, Γ, at the scatterer may be determined by applying the Lorentz reciprocity theorem [11] over the surface of the closed volume defined by S_1, S_2, S_3, and the cylindrical surface of infinite radius between S_1 and S_2. Denoting the scattered field by $\bar{E}^s$, $\bar{H}^s$, we have

$$\iint_{S_1+S_2+S_3} [\bar{E}^s \times \bar{H}^i - \bar{E}^i \times \bar{H}^s] \cdot \bar{n} da = 0 \qquad (1)$$

where the integral over the cylindrical surface of infinite radius vanishes because of exponential decay of the surface wave fields and the radiation condition. Since the scatterer is a perfect conductor $\bar{E}^i = -\bar{E}^s$ on S_3. Thus, the integral over S_3 takes the form

$$\iint_{S_3} [\bar{E}^s \times (\bar{H}^i + \bar{H}^s)] \cdot \bar{n} da \qquad (2)$$

Because of the orthogonality relations [12], [13] between the surface wave modes and the radiation

[1] For details of the dielectric image line and measurement of scatterer impedance, see [5].

field, the only component of the scattered field $\overline{E}^s$, $\overline{H}^s$ which contributes to the integration over S_1 and S_2 is a surface mode of the same type as the incident wave. Moveover, only the transverse components of the surface mode apply in (1), hence we express the transverse components of the incident surface wave in the form

$$\overline{E}_t{}^i e^{-j\zeta z}$$
$$\overline{H}_t{}^i e^{-j\zeta z}. \tag{3}$$

The transverse components of the scattered field propagating in the negative z direction are

$$\Gamma\overline{E}_t{}^i e^{+j\zeta z}$$
$$-\Gamma\overline{H}_t{}^i e^{+j\zeta z} \tag{4}$$

and for the positive z direction are

$$A\overline{E}_t{}^i e^{-j\zeta z}$$
$$A\overline{H}_t{}^i e^{-j\zeta z} \tag{5}$$

where $\overline{E}_t{}^i$, $\overline{H}_t{}^i$ are transverse field vectors normal to the z axis, ζ is the axial propagation constant, Γ is the reflection coefficient for the wave propagating in the negative z direction, and A is a similar coefficient for the positive z direction.

When the field expressions (3) and (5) are substituted into (1) in order to evaluate (1) over the surface S_2, the integrand of (1) is identically zero. Only integration over surfaces S_1 and S_3 contributes to (1). Thus, substituting (3) and (4) into (1), with (2) as the form of (1) over surface S_3, (1) reduces to

$$2\Gamma\iint_{S_1}\overline{E}_t{}^i\times\overline{H}_t{}^i\cdot\bar{n}da=-\iint_{S_3}\overline{E}^s\times(\overline{H}^i+\overline{H}^s)\cdot\bar{n}da.$$

Note that the exponential factors in (3) and (4) vanish in this expression. Hence, the complex reflection coefficient Γ at the scatterer is given by

$$\Gamma=\frac{-\frac{1}{2}\iint_{S_3}\overline{E}^s\times(\overline{H}^i+\overline{H}^s)\cdot\bar{n}da}{\iint_{S_1}\overline{E}_t{}^i\times\overline{H}_t{}^i\cdot\bar{n}da}\cdot \tag{6}$$

The density of current $\overline{J}^s$ on the surface of the scatterer is equal to $\bar{n}\times(\overline{H}^i+\overline{H}^s)$ where $(\overline{H}^i+\overline{H}^s)$ is the *total* magnetic field on S_3. The scattered field produced by this current is $\overline{E}^s$.

We shall now consider the scatterer as a surface wave launcher (*i.e.*, a source). The efficiency of a launcher is defined as

$$\eta=\frac{\text{surface wave power}}{\text{total power input to launcher}}=\frac{P_{sw}}{P_{\text{total}}}\cdot \tag{7}$$

If the current distribution on S_3 as a source is identical to $\overline{J}^s$ of the scatterer, then the field produced by the launcher is identical to the field $\overline{E}^s$ of the scatterer. Thus, the total power input to the launcher is given by

$$P_{\text{total}}=\frac{1}{2}\,Re\iint_{S_3}\overline{E}^{s*}\times(\overline{H}^i+\overline{H}^s)\cdot\bar{n}da \tag{8}$$

where $\overline{E}^s$ is the field produced by the source current $\overline{J}^s=\bar{n}\times(\overline{H}^i+\overline{H}^s)$ on the imaginary surface S_3 but with the perfectly conducting metal launcher removed. The asterisk (*) denotes the standard operation of taking the conjugate of a complex quantity.

Assuming the field is symmetric about the launcher, the total power in the surface wave propagating in the positive and negative z directions is equal to twice the power in the negative z direction. Thus, we write

$$P_{sw}=2\left[\frac{1}{2}\,Re\iint_{S_1}\overline{E}^s\times\overline{H}^{s*}\cdot(-\bar{n})da\right] \tag{9}$$

where only the surface wave part of the scattered field $\overline{E}^s$, $\overline{H}^s$ applies in (9). As with (1), the form of (9) requires only the transverse components of the field. Substituting (4) into (9) yields

$$P_{sw}=|\,\Gamma\,|^2\,Re\iint_{S_1}\overline{E}_t{}^i\times\overline{H}_t{}^{i*}\cdot\bar{n}da \tag{10}$$

where the exponential factors of (4) cancel when the complex conjugate of $\overline{H}_t{}^i$ is taken.

Substituting (8) and (10) into (7) gives the expression for launching efficiency as

$$\eta=\frac{|\,\Gamma\,|^2\,Re\iint_{S_1}\overline{E}_t{}^i\times\overline{H}_t{}^{i*}\cdot\bar{n}da}{\frac{1}{2}\,Re\iint_{S_3}\overline{E}^{s*}\times(\overline{H}^i\times\overline{H}^s)\cdot\bar{n}da}\cdot \tag{11}$$

We wish to remove the conjugate asterisks (*) appearing in (11). First consider the integral over surface S_1. Since $\overline{E}_t{}^i$ and $\overline{H}_t{}^i$ are in time phase, they may be defined to be real vector functions of the transverse coordinates. Thus, the conjugate sign may be removed from $\overline{H}_t{}^i$ in the integral. Moreover, the integral over S_1 is now a real quantity so the Re sign before the integral may be removed.

Next consider the integral over surface S_3. On S_3, $\overline{E}^s=-\overline{E}^i$. If the axial dimension of the launcher is quite small, then the integration over S_3 may be taken as entirely in the transverse plane. Therefore, only the transverse component of $\overline{E}^s$ contributes to the integral, and the substitution of $-\overline{E}_t{}^i e^{-j\zeta z}$ for $\overline{E}^s$ in (11) is valid. Since $\overline{E}_t{}^i$ is real and $e^{-j\zeta z}\approx 1$ at $z=0$ for $z/\lambda\ll 1$, the conjugate sign may be removed from $\overline{E}^s$. Hence (11) may be written in the form

$$\eta=\frac{|\,\Gamma\,|^2\iint_{S_1}\overline{E}_t{}^i\times\overline{H}_t{}^i\cdot\bar{n}da}{\frac{1}{2}\,Re\iint_{S_3}\overline{E}^s\times(\overline{H}^i\times\overline{H}^s)\cdot\bar{n}da}\cdot \tag{12}$$

Comparing (6) and (12) we see that

$$\eta = \frac{|\Gamma|^2}{-Re\ \Gamma}. \tag{13}$$

Note that Γ in this equation is the reflection coefficient at $z=0$ for the *composite* load of the scatterer and the infinite surface waveguide to the right. It is preferable to express efficiency in terms of a measurable parameter which represents just the scatterer and *not* the scatterer plus the infinite surface guide. Consider the particular case of the dielectric image line where one measures the normalized shunt impedance, z, of the scatterer, by placing a short circuit plate an odd multiple of $\lambda_g/4$ to the right of the scatterer [5]. This isolates the scatterer from the dielectric rod to the right of $z=0$ and allows greater accuracy in the standing wave measurements. Therefore, rewriting (13) in terms of the normalized shunt impedance z of the scatterer alone, one obtains

$$\eta = \frac{1}{1 + \left\{\begin{matrix}2\\1\end{matrix}\right\} Re\ z}. \tag{14}$$

Eq. (14) is valid under the following conditions:

[The current distribution on the launcher when used as a source is identical to the current distribution on the launcher when it appears as a scatterer on the surface waveguide.] (15a)

[The axial dimension of the launcher is very small compared to the wavelength.] (15b)

In a similar manner it may be shown that the launching efficiency of a slot or aperture in a perfectly conducting transverse sheet is given by

$$\eta = \frac{1}{1 + \left\{\begin{matrix}2\\1\end{matrix}\right\} Re\ y} \tag{16}$$

where y is the normalized shunt admittance of the slot or aperture. Eq. (16) is valid under the following conditions:

[The electric field distribution in the slot when it is used as a source is identical to the field distribution in the slot when it appears as a scatterer on the surface waveguide.] (17a)

[The axial dimension of the aperture is very small compared to the wavelength.] (17b)

In the above equations, the factor two should be used for bidirectional launching. If a short circuit plate is placed an odd multiple of $\lambda_g/4$ to one side of a wire launcher, or if a cavity is placed on one side of a slot launcher (*i.e.*, unidirectional launching is obtained), then the factor one in (14) and (16) must be used. In all of the results to follow, only unidirectional launching is considered.

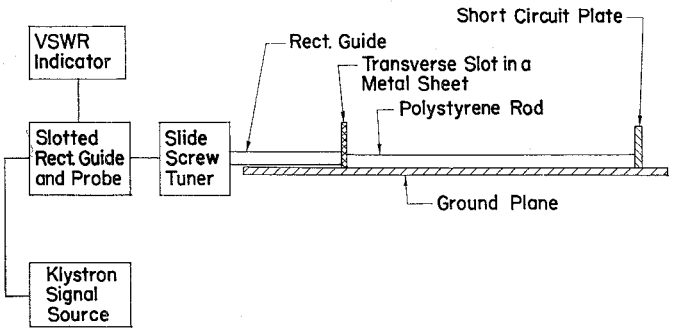

Fig. 3—The equipment used to measure the scattering matrix coefficients of a slot launcher.

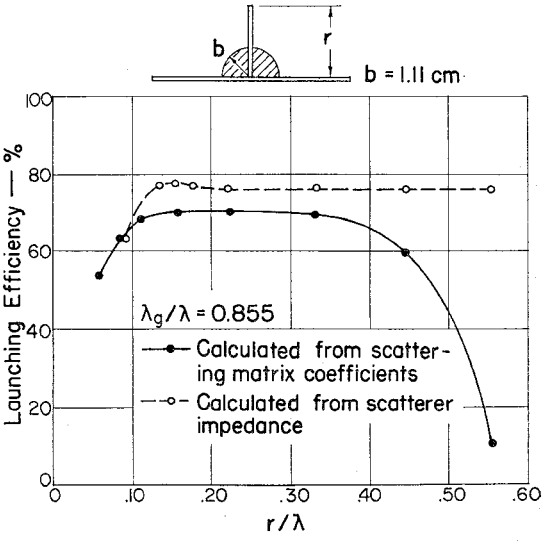

Fig. 4—Launching efficiency of a vertical wire.

Launching Efficiency from Scattering Matrix Coefficients

In several cases a slot or wire launcher was excited from rectangular waveguide and was the source of the surface wave on the image line. For example, excitation of a slot launcher is illustrated in Fig. 3. Efficiency was determined by considering the transition from rectangular waveguide to surface guide through the launcher as a two-port waveguide junction. The scattering matrix coefficients of the launcher were determined by Deschamps' method [14], [15] and the "matched" efficiency was calculated from the coefficients [16]. This method provided a direct measurement of efficiency under operating conditions where the launcher was the source of the surface wave. It was used to check the validity of efficiency as predicted from the scatterer impedance.

A comparison of efficiency by the two methods is illustrated in Fig. 4 for a vertical wire or monopole. The monopole was excited from rectangular waveguide which was mounted below the ground plane. The results agree within 6 per cent for wire lengths less than 0.35λ.

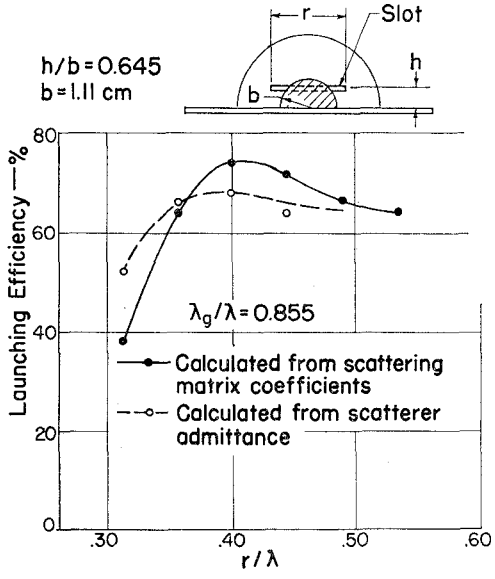

Fig. 5—Launching efficiency of a horizontal slot above the ground plane.

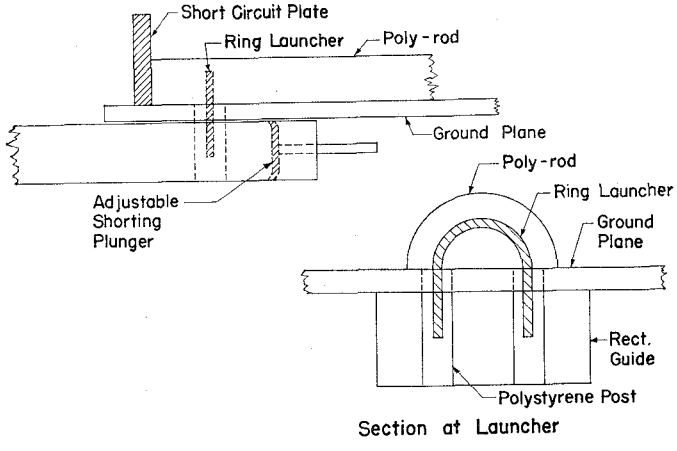

Fig. 6—Excitation of ring launcher from rectangular waveguide.

Efficiency calculated from the scatterer impedance is in serious error for wires longer than 0.35λ. This is because condition (15a) was not satisfied by long wire launchers.

A slot launcher was constructed by milling a narrow slot in a large, thin brass sheet. The slot was above, and parallel to, the ground plane. It was excited from rectangular waveguide as shown in Fig. 3. The variation of launching efficiency with slot length is illustrated in Fig. 5. The two methods yielded results which were within reasonable agreement. If the slot length is small compared to the wavelength, then condition (17a) will usually be satisfied and efficiency calculated from the scatterer admittance should be accurate.

A ring launcher was excited from rectangular guide below the ground plane. Details of this launcher are shown in Fig. 6. A balanced, symmetric excitation of the ring was necessary because the field distribution of the dipole mode requires a current null at the top of the ring. The mean ring radius was 0.715 cm. A comparison of results for this launcher is given in Table I.

TABLE I

λ_g/λ	Frequency mc	Normalized Ring Radius	Per Cent Efficiency Predicted from the Scatterer Impedance	Per Cent Efficiency Measured by Scattering Matrix Method
0.818	7436	0.177	82.3	82
0.897	5928	0.141	80.6	78

Experimental Results

Launching efficiency as a function of launcher dimensions is presented for the vertical monopole, ring, annular slot, and horizontal slot. The efficiency was calculated from the measured scatterer impedance. Unidirectional launching, as well as the satisfaction of conditions (15) or (17), was assumed. The practical problem of obtaining unidirectional launching is discussed in a later section.

Scatterer impedance was measured at six values of λ_g/λ extending from 0.818 to 0.987. Two efficiency curves for each launcher are presented, and they are for λ_g/λ equal to 0.818 and 0.897 which correspond to b/λ equal to 0.275 and 0.22, respectively. Measurements were performed in the frequency range of 5900 to 7400 mc. Surface wave attenuation due to dielectric loss [8] introduced a slight error in the measured impedance of a scatterer. This occurred because of the lossy guide between the measuring probe and scatterer. The effect of the attenuation on efficiency calculations was negligible. In the results presented here, the rod was assumed lossless and no correction was applied to the impedance measurements.

Fig. 7 illustrates the efficiency of a vertical wire or monopole as a function of the normalized wire length. The wire was silver tubing 0.15 cm in diameter and was oriented perpendicular to the ground plane. Fig. 8 shows the launching efficiency of a ring as a function of the normalized ring radius. The ring was positioned concentrically about the rod axis. The radial width of the ring was 0.16 cm and its axial thickness was 0.08 cm. Fig. 9 illustrates the efficiency of an annular slot in a thin metal sheet. The slot was concentric with the rod axis. For this case and all other slot launchers, the slot width was 0.16 cm and the metal sheet thickness was 0.08 cm. Fig. 10 illustrates the launching efficiency of a horizontal slot as a function of the normalized slot length. The slot was located above the ground plane at a normalized height $h/b=0.645$. The manner in which slot height affects the efficiency of a horizontal slot is shown in Fig. 11. Results were obtained only at $\lambda_g/\lambda=0.818$. The data are for resonant slots where the scatterer admittance was a pure conductance. The resonant slot length varied slightly for the different measurements but was always about 14 mm which yields $r/\lambda\approx 0.35$. The normalized slot height h/b appears along the abscissa of the graph. The optimum height was quite critical, and maximum efficiency of 80 per cent was obtained when $h/b=0.72$.

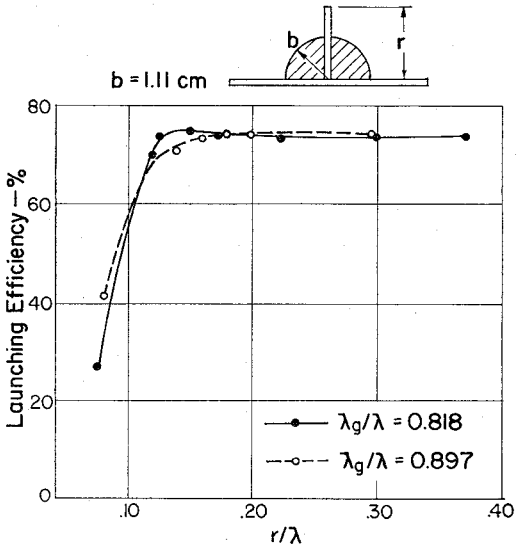

Fig. 7—Launching efficiency of a vertical wire as a function of the normalized wire length.

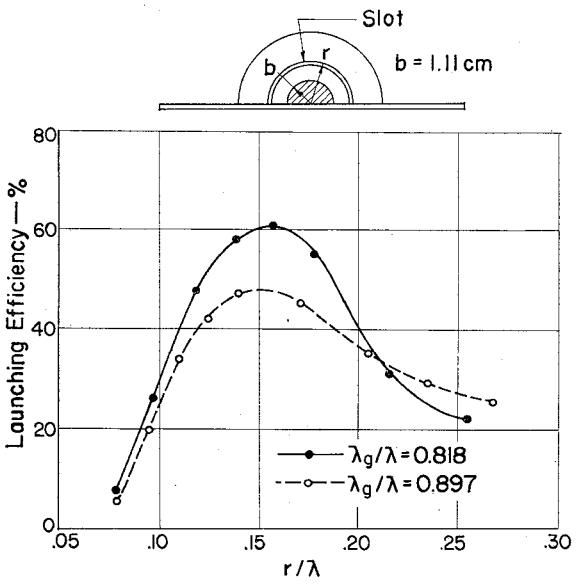

Fig. 9—Launching efficiency of an annular slot as a function of the normalized slot radius.

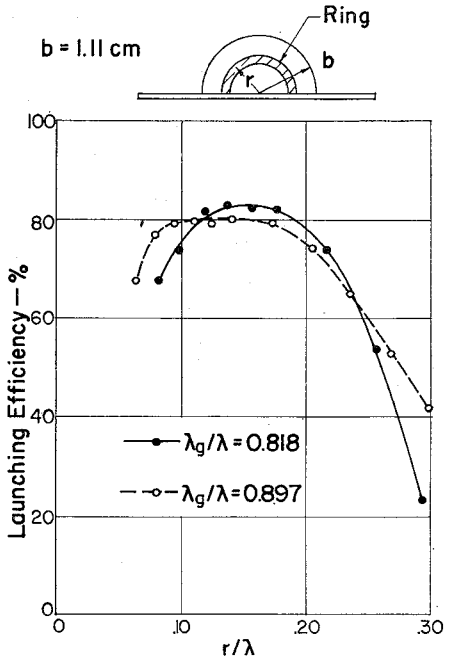

Fig. 8—Launching efficiency of a ring as a function of the normalized ring radius.

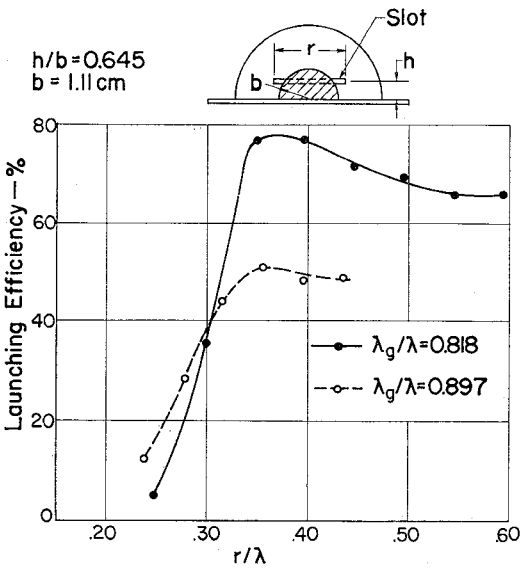

Fig. 10—Launching efficiency of a horizontal slot as a function of the normalized slot length.

The effect of surface wave coupling on launching efficiency is illustrated by the curves of Fig. 12 which show the efficiency of a resonant launcher as a function of λ_g/λ. Efficiency was always calculated when the dimensions of the launcher were such that its impedance or admittance as a scatterer was a real quantity. The largest efficiency was always obtained at the smallest λ_g/λ (largest b/λ). As λ_g/λ approaches unity, the surface wave is only slightly bound to the rod and the efficiency of a source decreases considerably. This effect was particularly evident with the annular slot where the efficiency at $\lambda_g/\lambda = 0.987$ was less than $\frac{1}{2}$ of the value at $\lambda_g/\lambda = 0.818$.

Unidirectional Launching

Unidirectional launching has been assumed in presenting the efficiencies for various types of launchers. For slot type launchers, this is readily accomplished by placing a cavity on one side of the slot or feeding the slot with a waveguide. If the presence of a cavity or waveguide does not disturb the field distribution in the slot (which is usually the case for slot sizes near resonance), then the launching efficiency will be very close to that predicted by the scatterer measurements.

However, for wire launchers it is necessary to place a reflecting device such as a reflecting plate or a parasitic element on one side of the launcher. The problem of required size for a reflecting plate was investigated for the

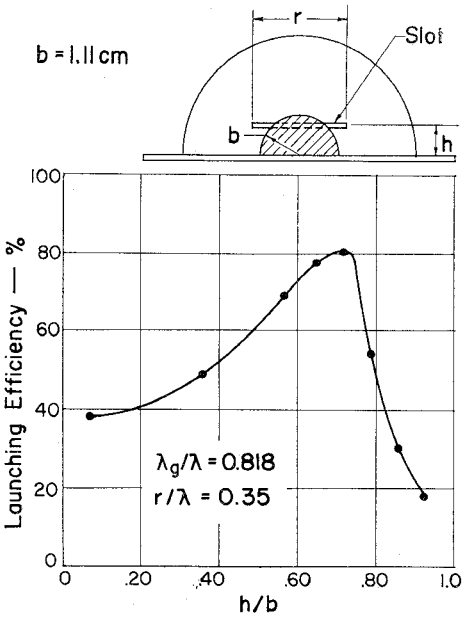

Fig. 11—Launching efficiency of a resonant horizontal slot as a function of the normalized slot height.

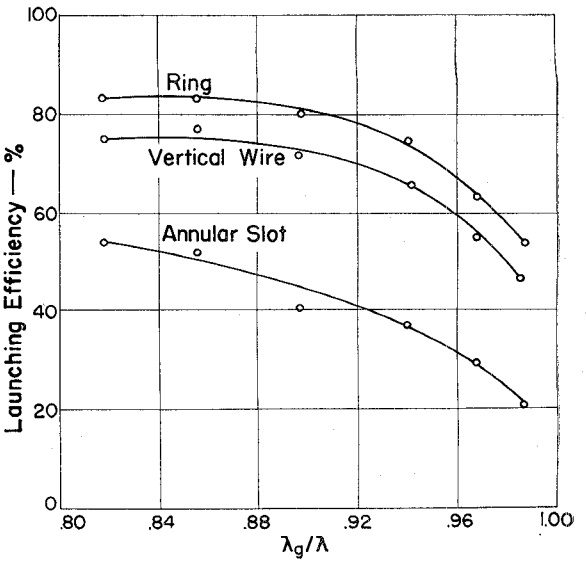

Fig. 12—Launching efficiency of a resonant launcher as a function of the parameter λ_g/λ.

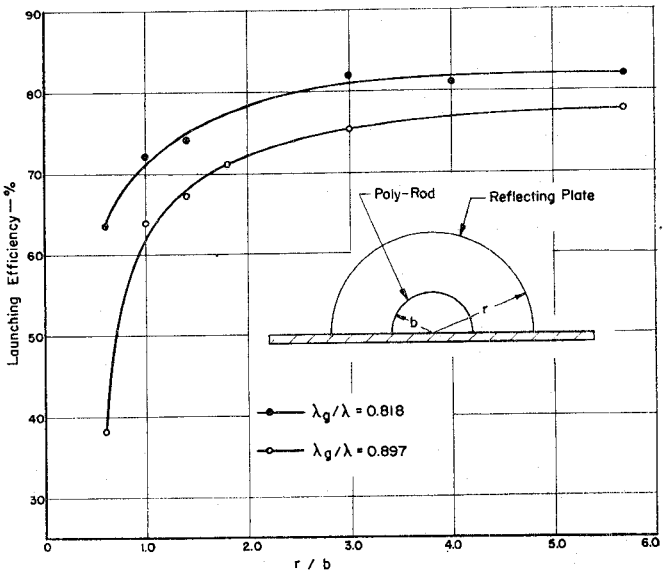

Fig. 13—Launching efficiency of a ring exciter as a function of the normalized reflecting plate radius.

case of a ring launcher at $\lambda_g/\lambda = 0.818$ and 0.897. Scattering matrix measurements of efficiency are shown in Fig. 13. The reflecting plates were very small in axial length, with a thickness of 0.17 cm and were spaced $\lambda_g/4$ from the ring. When the reflecting plate was reduced to the diameter of the rod, the ring efficiency decreased 11 per cent for the case $\lambda_g/\lambda = 0.818$ and 15 per cent for $\lambda_g/\lambda = 0.897$.

The use of a parasitic monopole, as a reflector, placed near a ring launcher was also investigated. For $\lambda_g/\lambda = 0.897$ and the spacing of the monopole from the ring equal to $0.25\lambda_g$, it was found that a monopole length of 0.148λ gave a forward to rear power ratio of 20 db. However, the launching efficiency of the ring decreased from 78 per cent for the case of a plate reflector to 59 per cent for the monopole reflector.

Conclusions

Of the two methods of measuring launching efficiency described, the one making use of the scatterer impedance is by far the most convenient and economical if more than several measurements are needed. The reasons for this are that only one measurement of scatterer impedance is required as compared to four measurements for the scattering matrix method and the fact that it is much easier to construct the scatterer form of a launcher than the actual form. The scatterer impedance may be determined from measurements on the surface waveguide or, if this is not feasible, from measurements in the waveguide feeding the surface waveguide. Of course, in this latter situation, it is necessary to calibrate the junction by some method such as Deschamps'. When a simple launcher is used as a scatterer, the feed terminals are altered; *i.e.*, the terminals of a wire launcher are shorted and the feed terminals of a slot launcher are open circuited. For example, by comparing the ring launcher of Fig. 6 and the ring scatterer of Fig. 8, it is seen that the scatterer form is much easier to fabricate than the actual form of the launcher.

The determination of launching efficiency from the equivalent scattering matrix coefficients is accurate for all types and sizes of launchers whereas the scatterer impedance method is accurate only for simple types of launchers where conditions (15) or (17) are satisfied. Both methods may be applied to other types of surface waveguides.

Launching efficiencies on the image line of 70 to 80 per cent may be obtained from the monopole, ring, and horizontal slot. All are convenient transitions from rec-

tangular waveguide to the image line. Their small size and simplicity may offset the greater efficiency that can be obtained with large and lengthy horns. Alternately, greater efficiencies with the monopoles or rings may be obtained by exciting several of them spaced at half-wavelength intervals along the rod.

Both the monopole and ring maintain good efficiency over a wide frequency range. In this respect they are superior to the horizontal slot.

Acknowledgment

The authors kindly appreciate the support of Wright Air Development Center and wish to thank Nicholas J. Kuhn and Robert L. Jones for assisting with the measurements

Bibliography

[1] Hondros, D., and Debye, P. "Elektromagnetische Wellen an dielektrischen Drähten," *Annalen der Physik*, Vol. 32 (1910), pp. 465–476.
[2] Carson, J. R., Mead, S. P., and Schelkunoff, S. A. "Hyper-Frequency Wave Guides—Mathematical Theory," *Bell System Technical Journal*, Vol. 15 (April, 1936), pp. 310–333.
[3] Beam, R. E., *et al.* "Final Report on Investigations of Multi-Mode Propagation in Waveguides and Microwave Optics," Army Signal Corps Contract No. W36-039, SC-38240, Microwave Laboratory, Northwestern University, Evanston, Ill., 1950.
[4] Kiely, D. G. *Dielectric Aerials*, "Methuen's Monographs on Physical Subjects," New York: John Wiley and Sons, Inc., 1953.
[5] Duncan, J. W., and DuHamel, R. H. "A Technique for Controlling the Radiation from Dielectric Rod Waveguides," IRE Transactions on Antennas and Propagation, Vol. AP-5 (July, 1957), pp. 284–289.
[6] Margerum, D. L. "The Excitation of Electromagnetic Waves on Dielectric Rods," M.S. Thesis, Department of Electrical Engineering, Northwestern University, Evanston, Ill., 1950.
[7] King, D. D., and Schlesinger, S. P. "Losses in Dielectric Image Lines," IRE Transactions on Microwave Theory and Techniques, Vol. MTT-3 (January, 1957), pp. 31–35.
[8] Elsasser, W. M. "Attenuation in a Dielectric Circular Rod," *Journal of Applied Physics*, Vol. 20 (December, 1949), pp. 1193–1196.
[9] King, D. D. "Properties of Dielectric Image Lines," IRE Transactions on Microwave Theory and Techniques, Vol. MTT-3 (March, 1955), pp. 75–81.
[10] ——. "Circuit Components in Dielectric Image Lines," IRE Transactions on Microwave Theory and Techniques, Vol. MTT-3 (December, 1955), pp. 35–39.
[11] Huxley, L. G. H. *The Principles and Practice of Wave Guides*, New York: The Macmillan Co., 1947, pp. 297–299.
[12] Goubau, G. "On the Excitation of Surface Waves," Proceedings of the IRE, Vol. 40 (July, 1952), pp. 865–868.
[13] Adler, R. B. "Waves on Inhomogeneous Cylindrical Structures," Proceedings of the IRE, Vol. 40 (March, 1952), pp. 339–348.
[14] Deschamps, G. A. "Determination of Reflection Coefficients and Insertion Loss of a Waveguide Junction," *Journal of Applied Physics*, Vol. 24 (August, 1953), pp. 1046–1050.
[15] Storer, J. E., Sheingold, L. S., and Stein, S. "A Simple Graphical Analysis of a Two-Port Waveguide Junction," Proceedings of the IRE, Vol. 41 (August, 1953), pp. 1004–1013.
[16] Altschuler, H. M., and Felsen, L. B. "Network Methods in Microwave Measurements," *Proceedings of Symposium on Modern Advances in Microwave Techniques*, Polytechnic Institute of Brooklyn, Brooklyn, N. Y. (July, 1955), pp. 299–300.
[17] DuHamel, R. H. and Duncan, J. W. "Launching Efficiency of Wires and Slots for a Dielectric Rod Waveguide,"Electrical Engineering Research Laboratory, Engineering Experiment Station, University of Illinois, Urbana, Ill., Antenna Laboratory Technical Report No. 24, August, 1957.

Microwave Switching by Crystal Diodes*

MURRAY R. MILLET†

Summary—**This paper gives the results of an investigation of the use of a microwave crystal as an RF switching element. Variation of a dc bias applied to the crystal will change its impedance, thereby providing an electronic control of microwave power. Empirical data are correlated with the physical structure of the crystal and its equivalent circuit to establish the frequency and power limitations of the switch. A comparison is also made of the switching properties of germanium and silicon crystals. Curves are given for predicting the switching capacity of any diode once its impedance has been normalized with respect to the characteristic impedance of the waveguide. Some methods are suggested for improving the bandwidth and power capacity of the crystal switch.**

Introduction

IN MANY applications the need arises for a fast acting waveguide switch to serve as either an on-off device or RF modulator. The conventional mechanical switch, either rotor or vane type, switches in milliseconds and also has the disadvantage of large size when physical volume is considered. The electronic switch of the ferrite type is smaller in size and has a switching time measured in microseconds. However, large peak powers are required to drive the solenoid, and the problem of holding a large coil current for the duration of a long pulse with fast rise and fall times introduces complexities. This paper describes an RF switch comprised of a crystal rectifier as the switching element. Because of the small time constant of the crystal and its low impedance there is evolved an electronic switch capable of switching in a fraction of a microsecond and requiring low driving power. The crystal switch may also serve as an RF modulator or variable attenuator.

The common use for crystal rectifiers at microwave frequencies is as a mixer or frequency converter in a heterodyne system.[1] When used as such, the local oscil-

* Manuscript received by the PGMTT, October 29, 1957; revised manuscript received, January 23, 1958.
† Philco Corp., Philadelphia, Pa.

[1] H. C. Torrey and C. A. Whitmer, "Crystal Rectifiers," McGraw-Hill Book Co., Inc., New York, N. Y., p. 153; 1948.